THE UNIVERSITY OF MICHIGAN

COLLEGE OF ENGINEERING
Department of Chemical and Metallurgical Engineering
Multi-phase Fluids Laboratory

Progress Report

EFFECT OF CAVITATION ON SPRAY FORMATION

Russell A. Nielsen
Douglas Reinhard
M. Rasin Tek
J. L. York

UMRI Project 2815

under contract with:

DELAVAN MANUFACTURING COMPANY
WEST DES MOINES, IOWA

administered by:

THE UNIVERSITY OF MICHIGAN RESEARCH INSTITUTE ANN ARBOR

February 1960

TABLE OF CONTENTS

LIST OF TABLES

LIST OF FIGURES

ABSTRACT

In order to study, explore, and evaluate the effect of cavitation on spray formation, a new type of cavitating venturi nozzle has been conceived, designed, constructed, and tested.

Experiments conducted with the nozzle indicate that cavitating performance may be obtained and duplicated. Whether at threshold of cavitation or beyond it, the implosion of vapor bubbles nucleated at the throat of venturi is shown to affect and perturb the jet issuing from the nozzle where the process of spray formation originates. Visual observations, metering and pressure data, and photographs of cavitation phenomena and of the jet are presented and discussed.

The hydraulics of flow through the venturi nozzle and design requirements for cavitating performance are included.

INTRODUCTION

Previous studies have indicated that unstable conditions may be induced by disturbances produced in a cavitating flow. The pronounced effect of surface instabilities on the formation and properties of sprays is well known. Work aimed at exploring the possibilities of producing better sprays by cavitating nozzles was initiated last summer. The initial experiments and theoretical studies were reported in our past progress reports. The encouraging results obtained during the preliminary investigations suggested expansion of the scope of experimentation into development of nozzles especially designed for cavitating performance, and collection of quantitative data along with photographs by short-exposure technique.

These early experiments performed to test the effect of cavitation on formation of sprays were aimed at producing a local region in the flow field where the pressure was to be lowered down to the vapor pressure of the liquid at its bulk temperature. The nucleation of vapor phase in the form of tiny bubbles in local areas of low pressure would be followed by implosion of the bubbles as they would be dragged by the main flow stream into regions of higher pressure. The degree of instability induced by the abrupt implosion of the cavity was expected to affect particle size and size distribution of the spray through the extremely intense energy release and local shock produced in the fluid.

The experiments on specially designed nozzles with high length-to-diameter ratios were described in the previous progress report. These experiments were conducted with liquid temperatures above the saturation temperature at atmospheric pressure. Consequently, considerable flashing occurred both at the nozzle exit and the low-pressure area immediately downstream from the flow obstructions. Under these conditions the detection and differentiation between cavitation and flashing becomes difficult. The high-frequency noise and vibration usually associated with cavitation phenomena becomes hard to discern when the noise of two-phase flow due to flashing is superimposed upon it. The recent experiments conducted with the high (L/D) ratio nozzles indicated that it is extremely difficult to reproduce and duplicate runs when cavitation and flashing are both present. For this reason the recent experiments were aimed at inducing cavitation with relatively cold feed so that no flashing would occur.

The work reported here includes the design and construction of a novel cavitating venturi nozzle and the experimental layout assembled and used during the experiments.

The discussion of the experiments includes observations on cavitating performance, pressure-flow data collected during the tests, and short-exposure photographs taken of the nozzle and the jet during several typical runs.

The studies of the hydraulics of flow through the venturi nozzle included metering characteristics, pressure and flow distributions, and calculations on the dimensionless cavitation number.

A summary of conclusions reached to date and recommendations for future work are included in the report.

The calculations of the pressure at the diffuser exit upstream from the orifice plate are included in an appendix.

EXPERIMENTAL

The use of a venturi in a nozzle was conceived as a result of our study of cavitation phenomena observed in performance of venturis. An article by B. S. Wright and S. D. Olicher, "Cavitating Venturi Flow Limiter" [Chem. Eng., 63, 221 (Nov., 1956)], reports work on the use of a cavitating venturi for liquid flow measurements. Cavitation was observed at the throat of the venturi with flowing cold water. Thus the installation of a specially designed venturi upstream of a spray device appeared to offer an excellent means for cavitation studies.

Figure 1 is a sketch of the venturi designed and constructed for this purpose. The venturi nozzle was built of Plexiglas to permit visual observations on cavitating performance. The diameter of the throat was 1/8 in. Four radial holes along a circumference and 90° apart were drilled and tapped as indicated

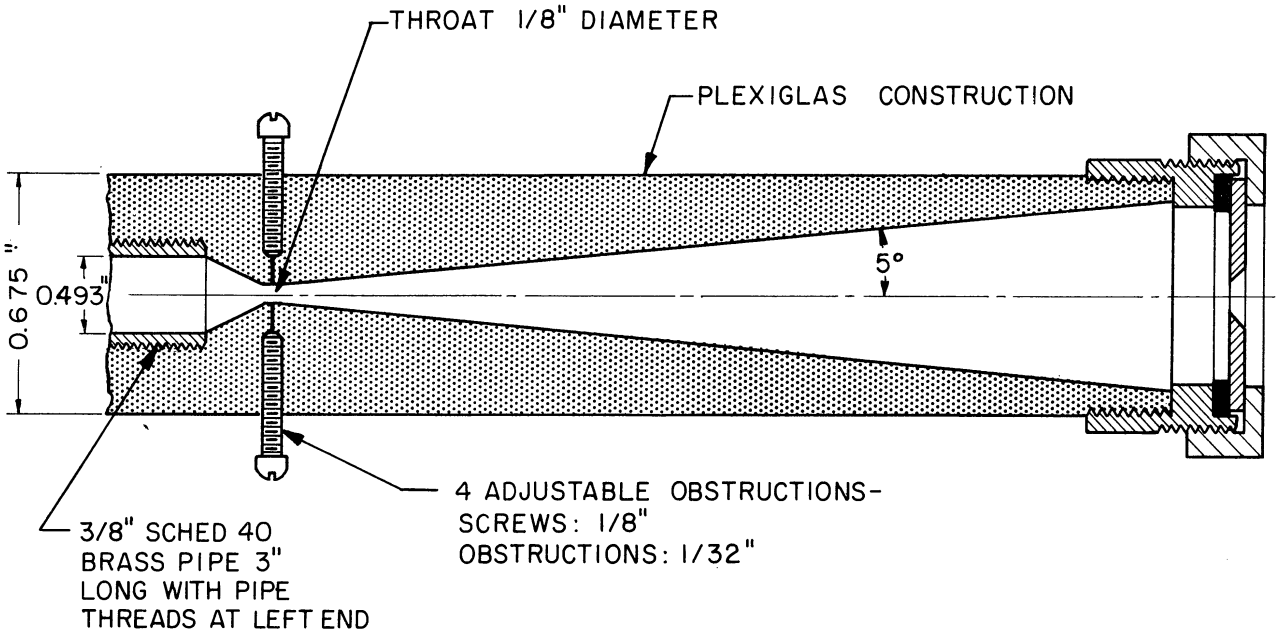

Fig. 1. Venturi nozzle assembly.

for assembly of flow obstructions. The taper angles of the converging and diverging sections of the venturi were set equal to 25 and 5°, respectively. To allow the greatest possible pressure recovery downstream from the throttle, the diffuser section was designed extra long for the initial experiments. The diffuser section was provided with an orifice plate at the exit. The experiments were started with a long diffuser section, which was to be shortened later, to provide data on the effect of distance between the cavitating section and the point of spray formation.

The inlet section, upstream from the throat, was designed with both tangential and axial entries.

One of the holes drilled and tapped for the installation of flow obstructions was used during some of the experiments as a pressure tap to measure the static pressure at the throat of the venturi. Four 3/32-in. machine screws to fit the holes were modified by soldering axially at the base of each screw a short piece of 1/32-in. piano wire ground flat at the ends. When assembled, these screws provided flow obstructions with variable depths of penetration into the throat of the venturi. The obstructions were designed to cause additional turbulence with localized low-pressure spots to induce cavitation.

The experimental layout is shown in Fig. 2. Pressure gauges were used to measure inlet and throat pressures. Temperature measurements were provided by a thermometer well immersed in the inlet stream. Temperature control was achieved by mixing hot and cold tap water. Throttling upstream of the inlet pressure gauge provided flow control. Flow measurement was done by weighing orifice effluent over a measured time interval.

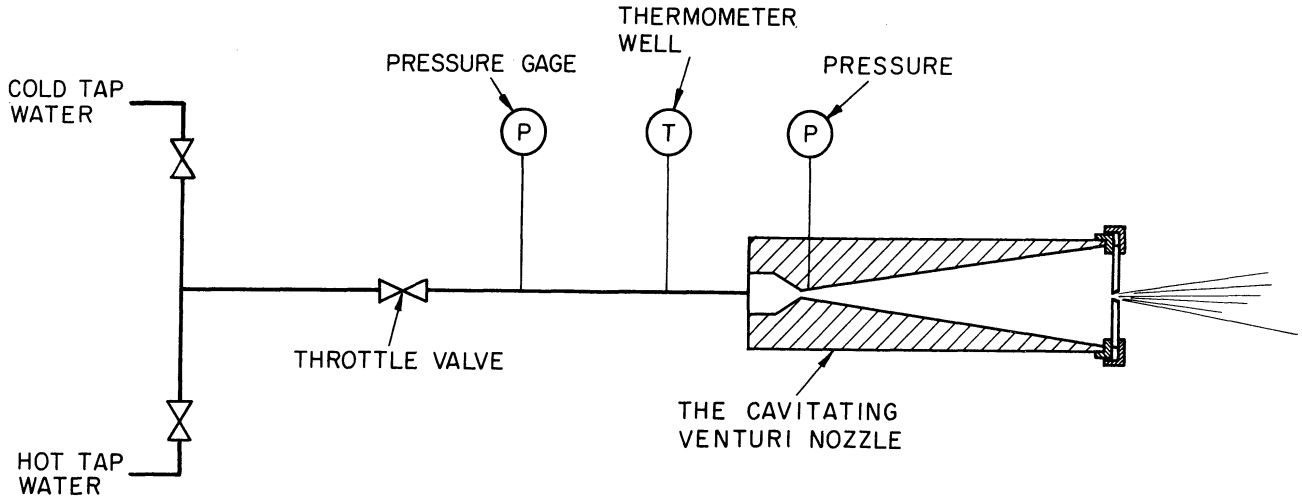

Fig. 2. Sketch of the experimental layout.

DISCUSSION OF EXPERIMENTS

Cavitation has been observed during a number of experimental runs. Under cavitating conditions a zone of two-phase flow develops at the throat and extends into the diffuser section of the venturi. The extent of the cavitation zone was affected by the pressure distribution near the throat of the venturi and the vapor pressure and velocity of the flowing fluid. Photographs of the cavitation zone and the jet issuing from the orifice have been taken for a range of the operating variables. Some typical photographs and the operating data collected are included in this report.

All the data collected to date were obtained with a full-length diffuser section (about 5 in.). Both axial and tangential liquid entries have been investigated with several sizes of orifice plates. Water inlet pressures of zero to 50 psig with a temperature range of from 45°F to 195°F represent the broad range of variables covered during the experiments.

Figures 3a, b, and c are photographs of the throat area of the nozzle. Figure 3a has been included to show the appearance of the throat area filled with stagnant water. Figures 3b and c show the increasing length of the cavitation zone caused by increasing flow rates. Cold water fed axially and a 3/16-in. orifice plate were used for these photographs. The cylindrical obstructions were set flush with the throat wall to eliminate their effect.

Figures 4a and b are similar photographs showing the lengthening of the cavitation zone caused by increasing water temperatures. A sharp-edged orifice of 0.205-in. diameter was used with obstructions again set at the wall. Water feed was axial.

Figures 5a and b are photographs taken of the throat area with protruding obstructions. Both photographs were taken with luke-warm axial water feed and a 3/16-in. orifice plate. Figure 5a shows the asymmetry introduced by a single protruding obstruction at right angles with the line of vision. Figure 5b shows the effect of two diametrically opposed obstructions perpendicular to the line of vision.

Photographs of the cold water jet issuing from a 0.205-in. orifice with axial feed are shown in Figs. 6a and b for low and high flow rates. Figures 6c and d are similar with warmer water. Obstructions were set flush with the wall. The striking waves at the surface of the jet in Fig. 6b contrast the relatively smooth surface of the jet of Fig. 6a. At high rates of flow, when the nozzle is cavitating more, the instability at the free surface of the jet is quite apparent.

Careful observation of Figs. 6c and 6d indicates clearly that at higher feed temperatures, with more cavitation, growing waves (Fig. 6c) and highly unstable

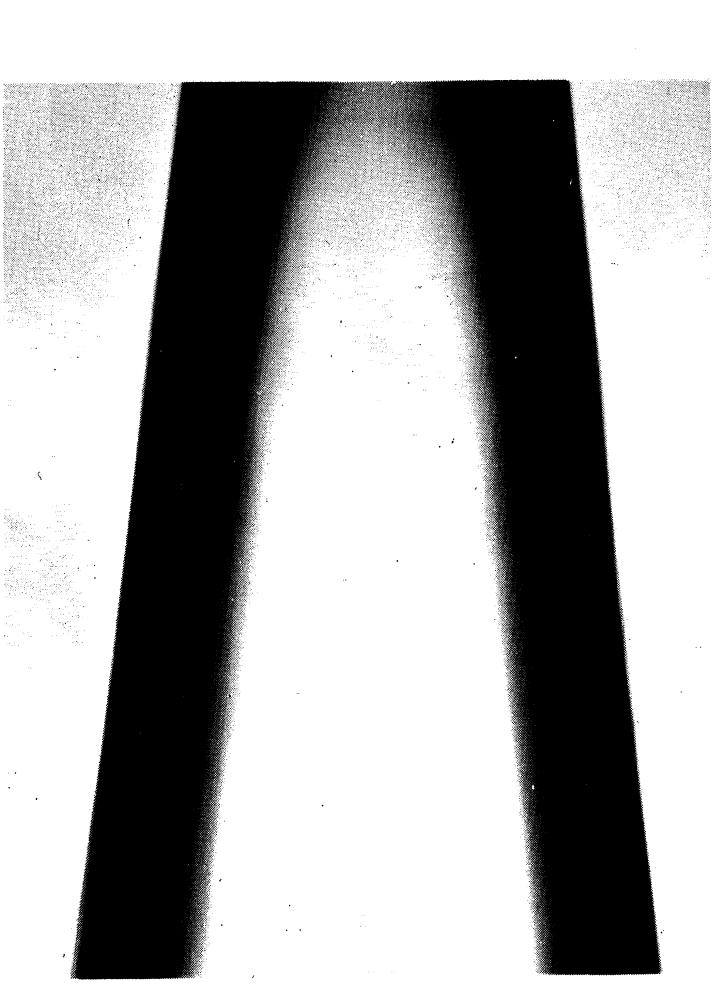

a. T = 57°F No flow (1)*

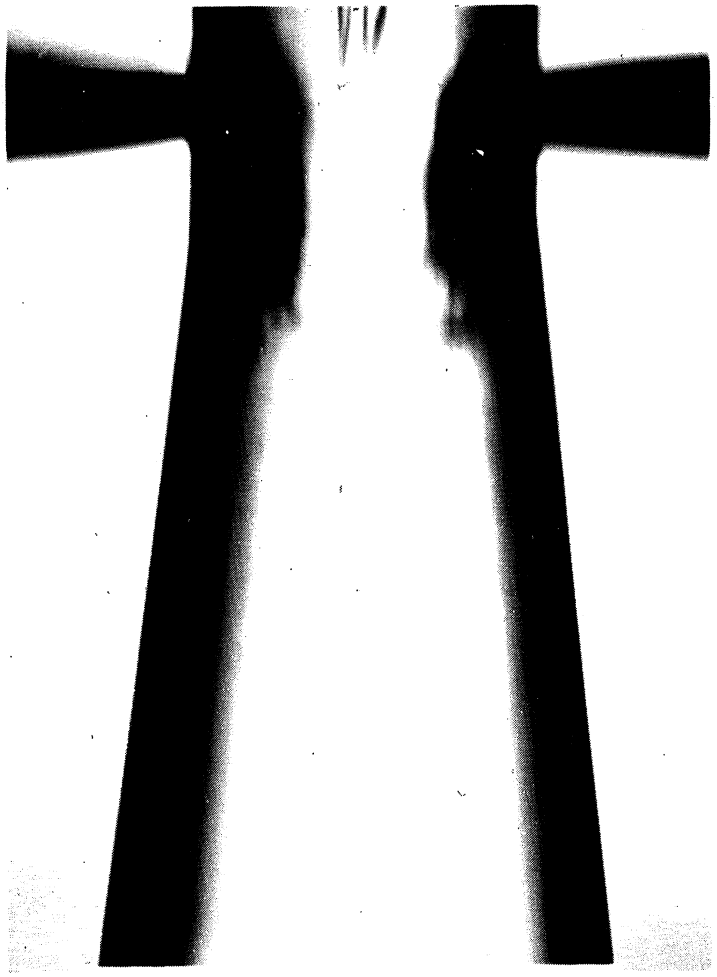

b. T = 57°F P_{in} = 10 psig (3)

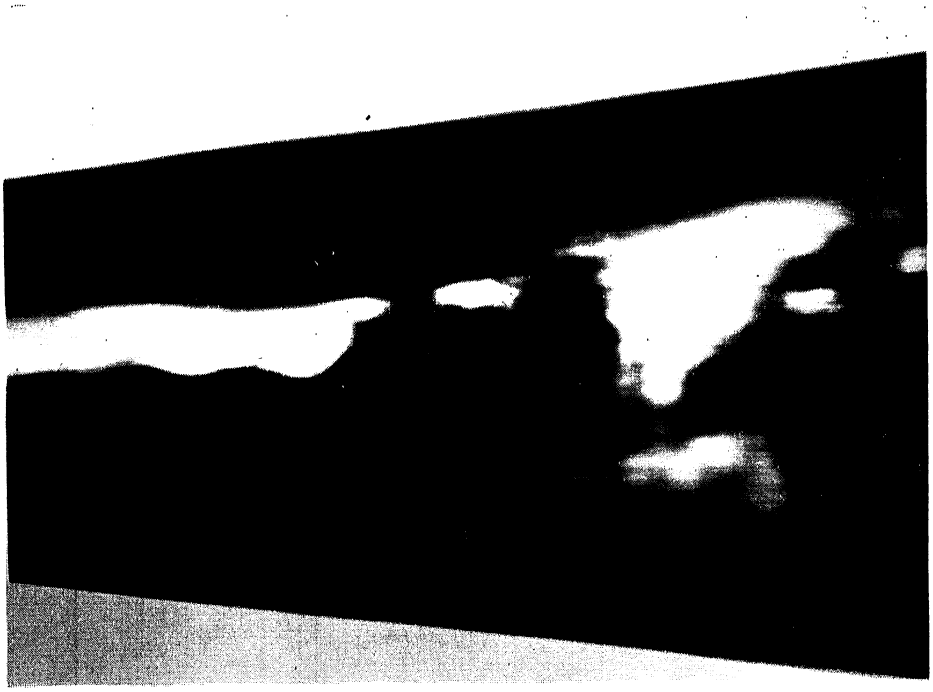

c. T = 57°F P_{in} = 45 psig (2)

Fig. 3. Photographs of the throat of the cavitating venturi nozzle.

*Numbers in parentheses are the negative numbers.

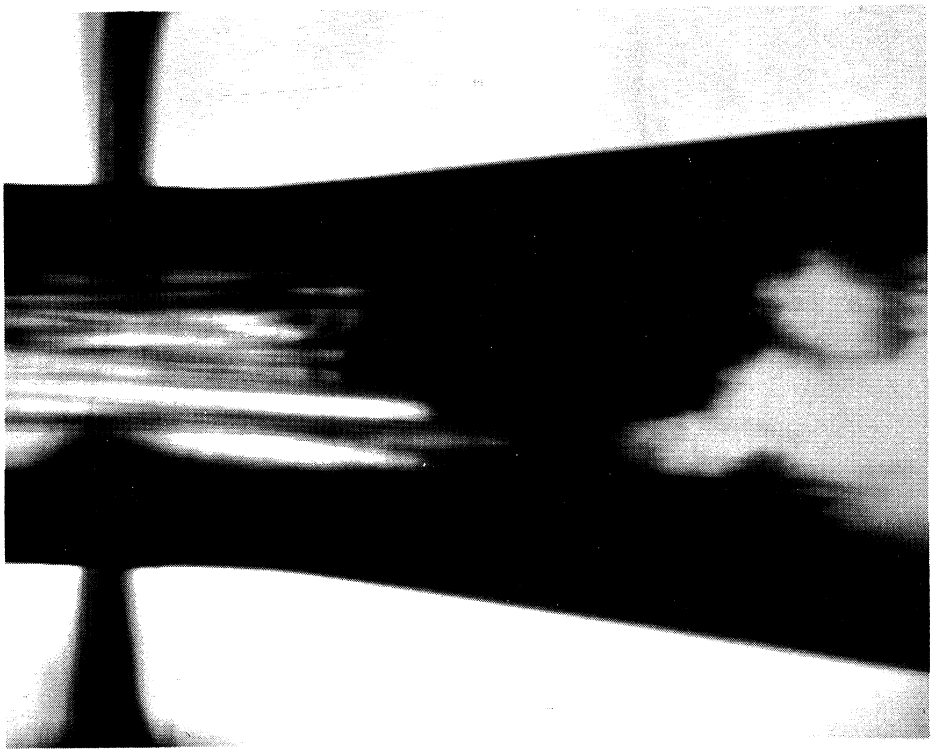

(11)

a. T = 46°F P_{in} = 24 psig

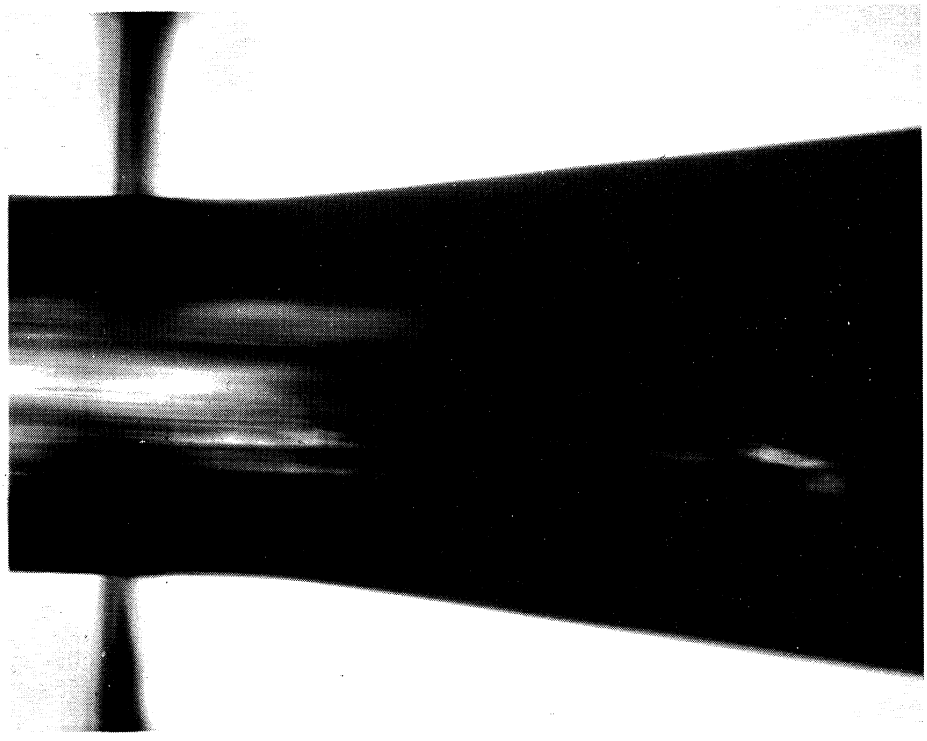

(13)

b. T= 154°F P_{in} = 24 psig

Fig. 4. Effect of water temperatures on the length of cavitating zone.

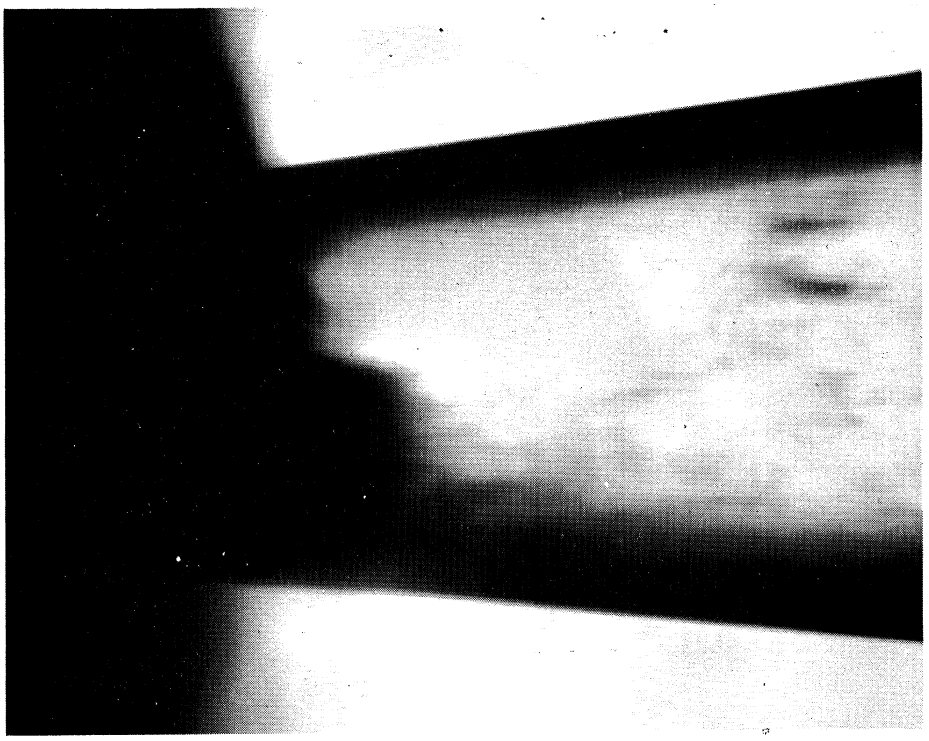

(9)

a. T = 95°F P_{in} = 25 psig
Assymetric flow obstruction at throat

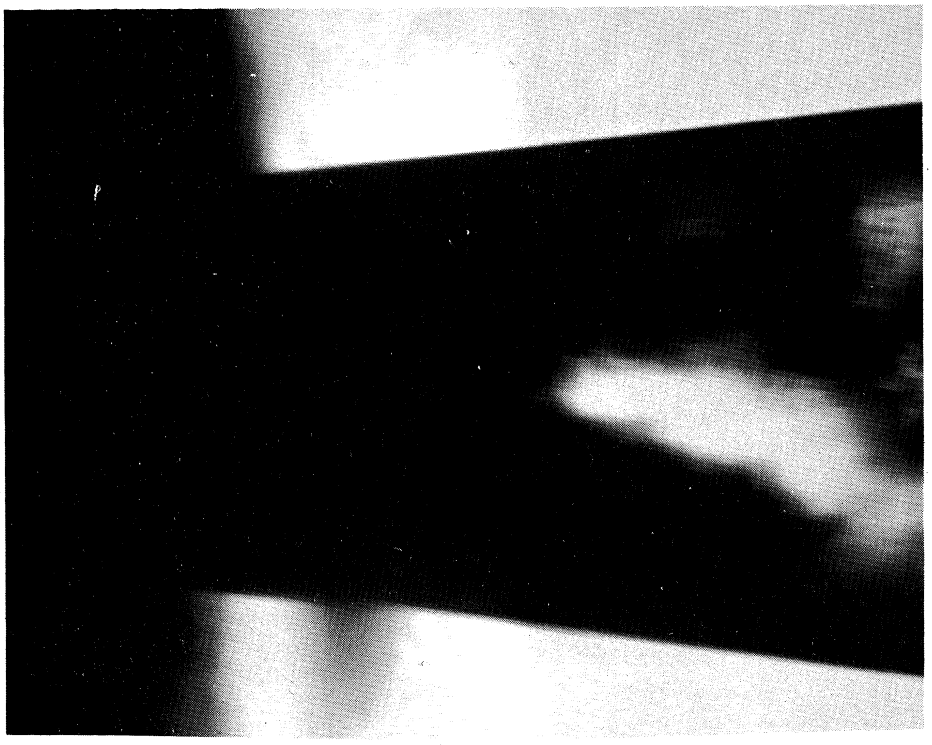

(10)

b. T = 95°F P_{in} = 25 psig
Two symmetrical flow obstructions

Fig 5. Effect of location of flow obstruction on the performance of cavitating venturi nozzle.

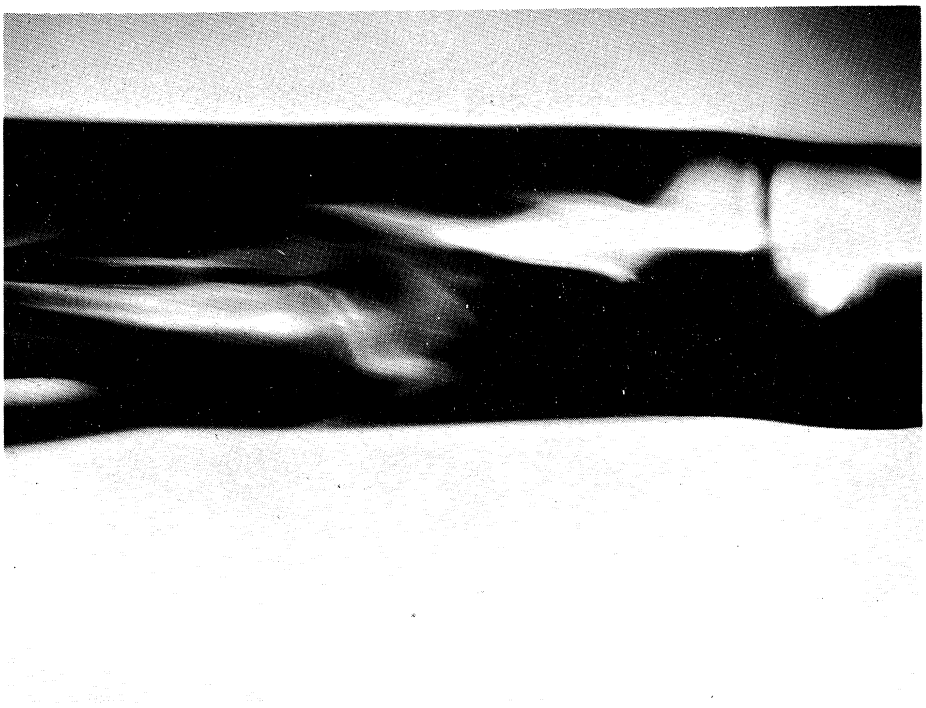

(14)

a. T = 44°F P_{in} = 10 psig

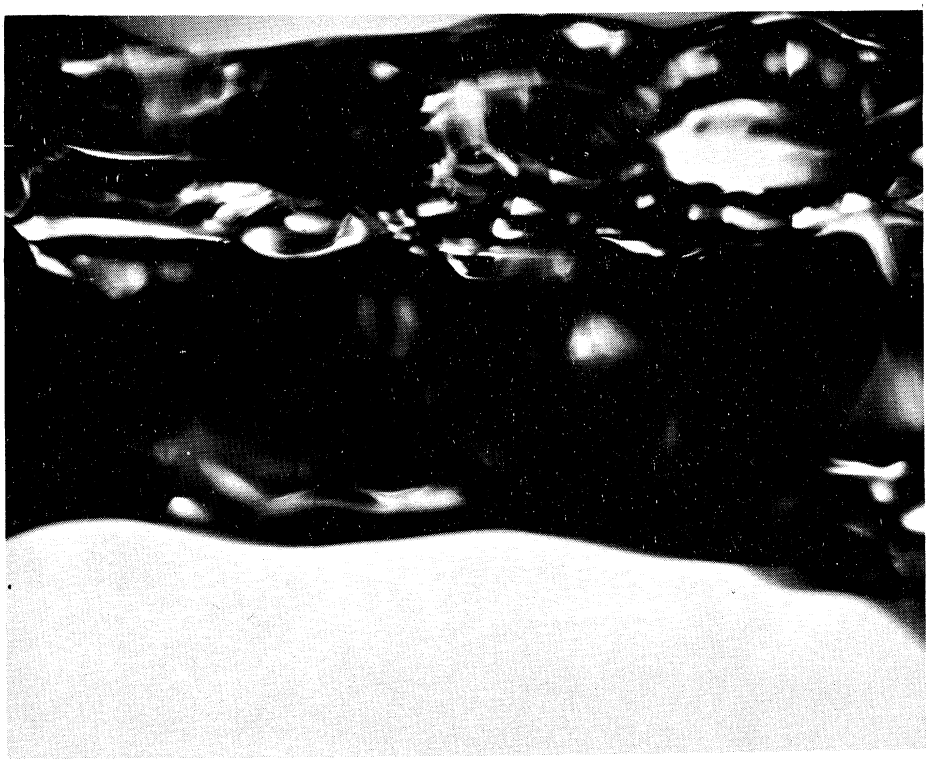

(16)

b. T = 44°F P_{in} = 40 psig

Fig. 6. Effect of cavitation (axial feed) on free surface of issuing jet.

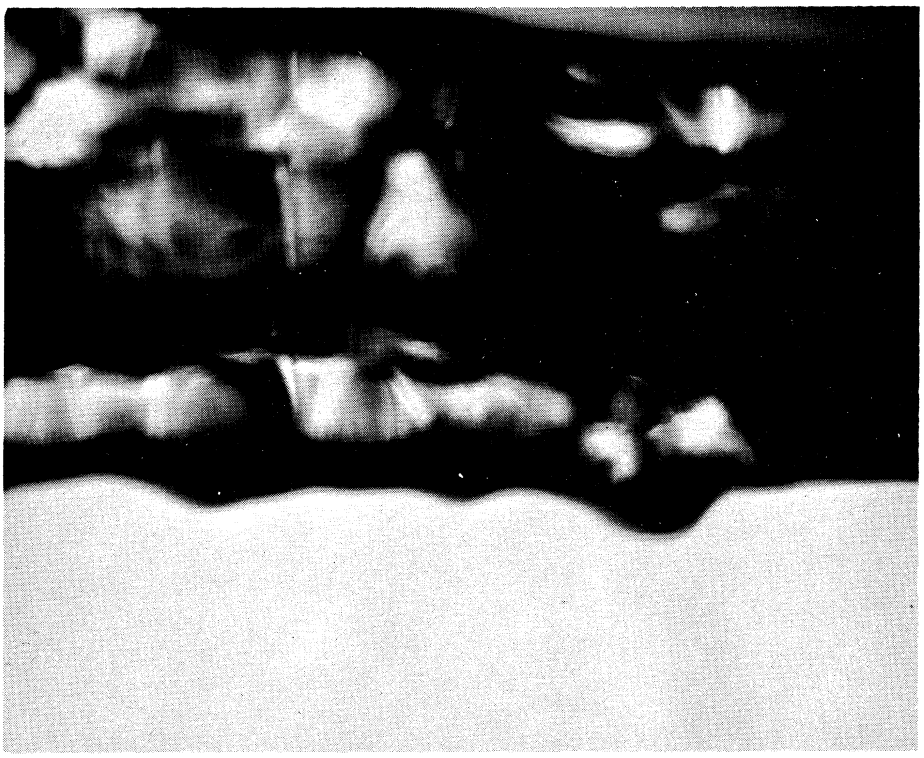

(17)

c. T = 140°F P_{in} = 10 psig

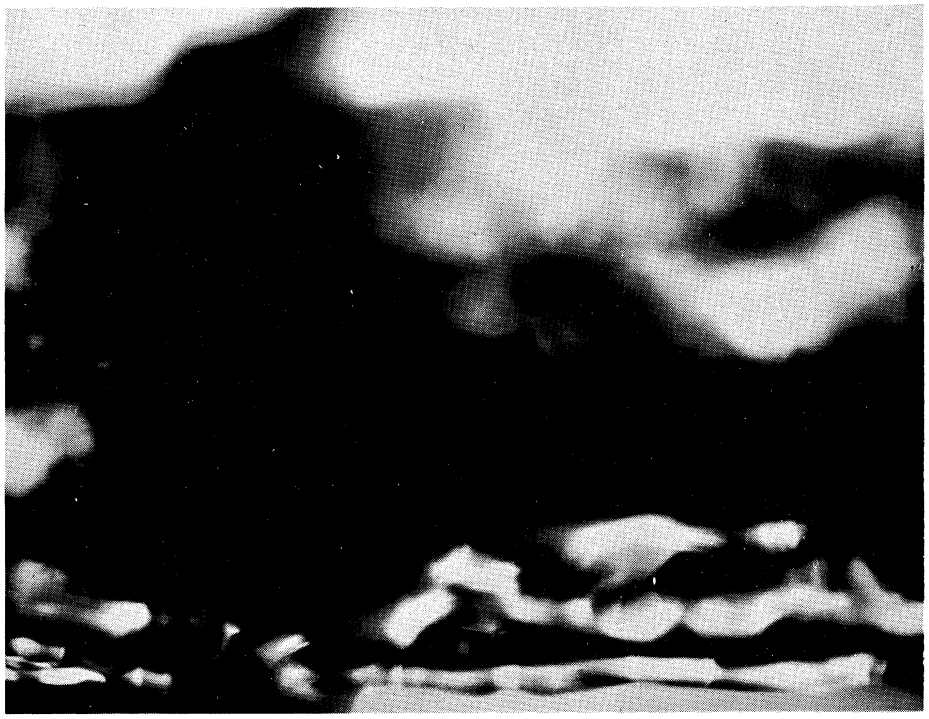

(19)

d. T = 140°F P_{in} = 40 psig

Fig. 6. (Concluded)

nonlinear effects (Fig. 6d) become present at the surface of the jet issuing from the nozzle.

The preceding photographs show the flame-like cavitation zone to be most dense near the wall of the throat and diffuser sections of the venturi. When water is fed tangentially, the cavitating zone was observed to move near the axis of the venturi. This effect is shown by the following series of photographs.

Figures 7a to d show the throat area of the venturi with tangential water feed and a 0.205-in. sharp-edged orifice at the exit. Figures 7a and b are of the throat area with cold water for both low and high flow rates; Figs. 7c and d, with warm water.

The orifice jet fans out conically when water is fed through the tangential entry device. Figures 8a to d show the jet issuing from a 0.205-in. sharp-edged orifice with tangentially fed water. Figures 8a and b are for cold water and Figs. 8c and d, for warm water.

The effect of cavitation in inducing unstable, growing waves at the surface of issuing conical sheet of water is strikingly apparent in these pictures.

A short series of photographs with tangential feed was taken during a period when the water was quite hot. Figures 9a and b are photographs of the throat area with hot water and a 0.205-in. orifice; Figs. 9c and d, with a 0.120-in. orifice.

Figures 9a, b, c, and d show the cavitation to be quite profuse near the throat. For the low flow rates, about 80% of the diffuser section was filled with two-phase fluid. For high flow rates, implosion occurs nearer to the throat but a considerable portion of the diffuser was still filled with two-phase fluid.

Photographs of the orifice jet were also taken for hot water entering tangentially. Figures 10a and b are photographs of the orifice effluent with a 0.205-in. plate.

Several series of experimental runs were made to obtain flow-rate and throat-pressure data over a range of inlet pressures and water temperatures. These data are presented in Table I for axial water feed and a 0.205-in. sharp-edged orifice.

For all runs with axial water feed, incipient cavitation was found to occur at a critical flow rate corresponding to an inlet pressure of about 10 psig. For lower flow rates no cavitation was observed. As the rate of flow was increased above this critical flow rate, cavitation was found to become more profuse with a correspondingly lower throat pressure.

Similar data are presented in Table II for tangential water feed and a 0.205-in. sharp-edged orifice.

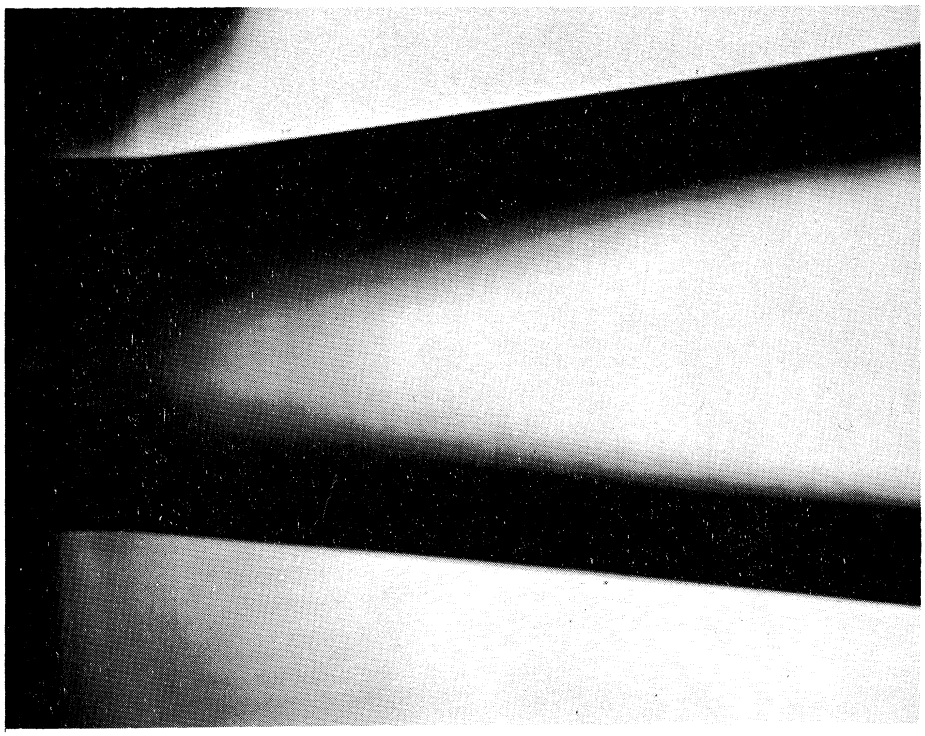

(20)

a. T = 48°F P_{in} = 10 psig

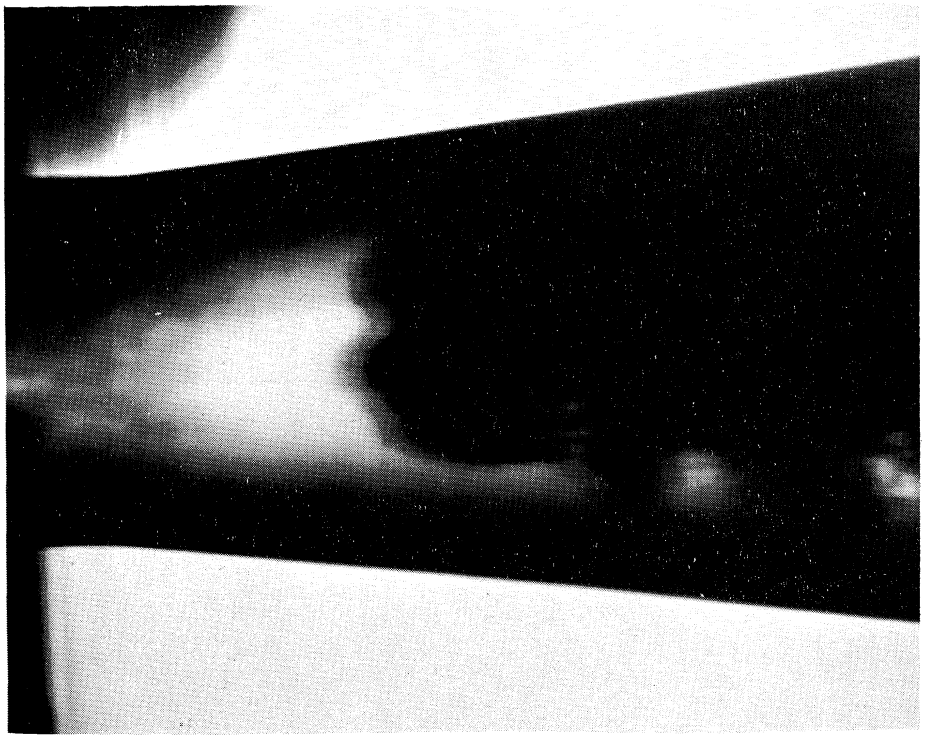

(22)

b. T = 47°F P_{in} = 40 psig

Fig. 7. Effect of flow rate and water temperature on cavitation (tangential feed).

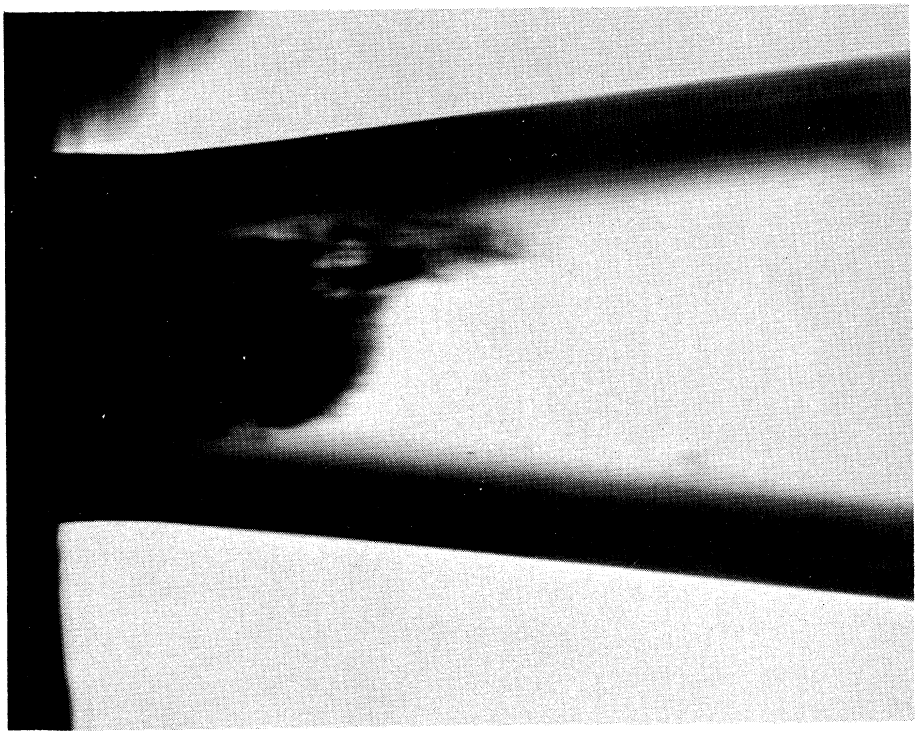

(23)

c. T = 132°F P_{in} = 10 psig

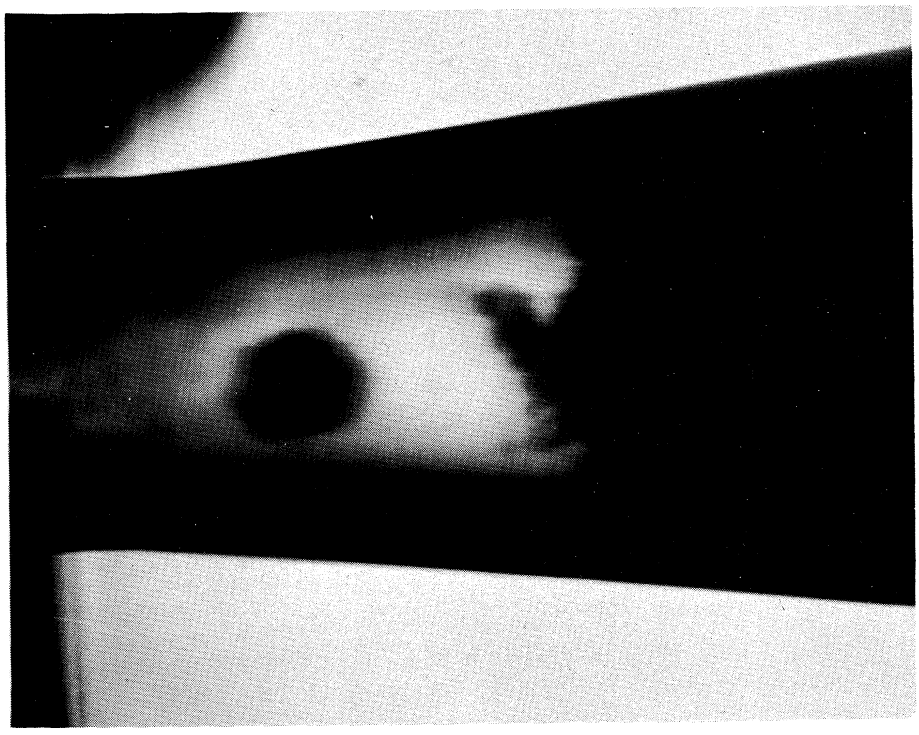

(25)

d. T = 132°F P_{in} = 40 psig

Fig. 7. (Concluded)

(31)

a. T = 48°F P_{in} = 10 psig

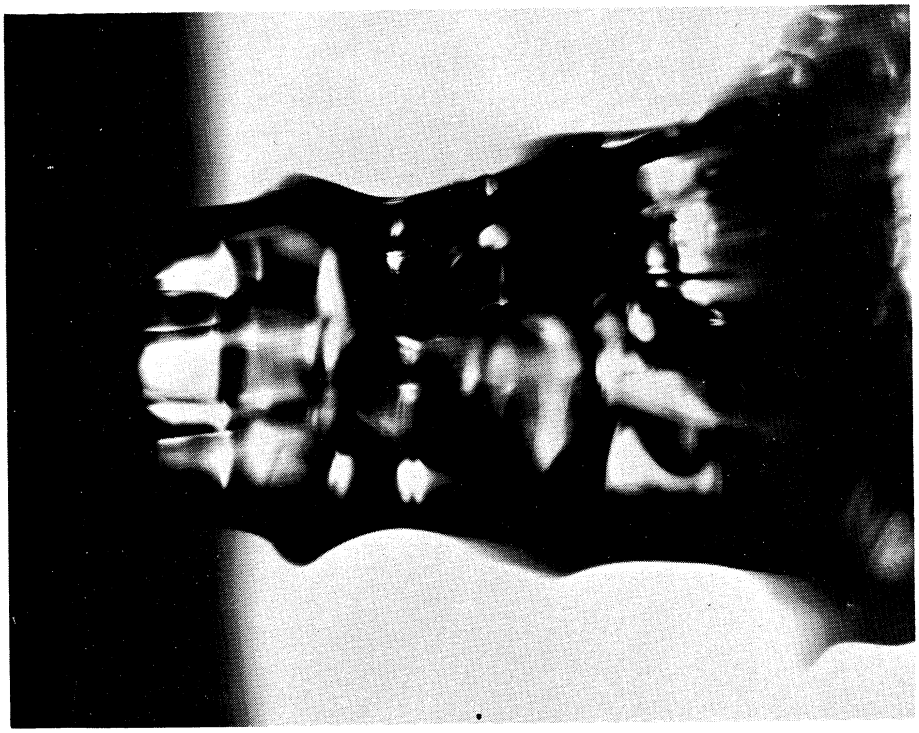

(29)

b. T = 48°F P_{in} = 40 psig

Fig. 8. Effect of cavitation on free surface of issuing jet (tangential entry)

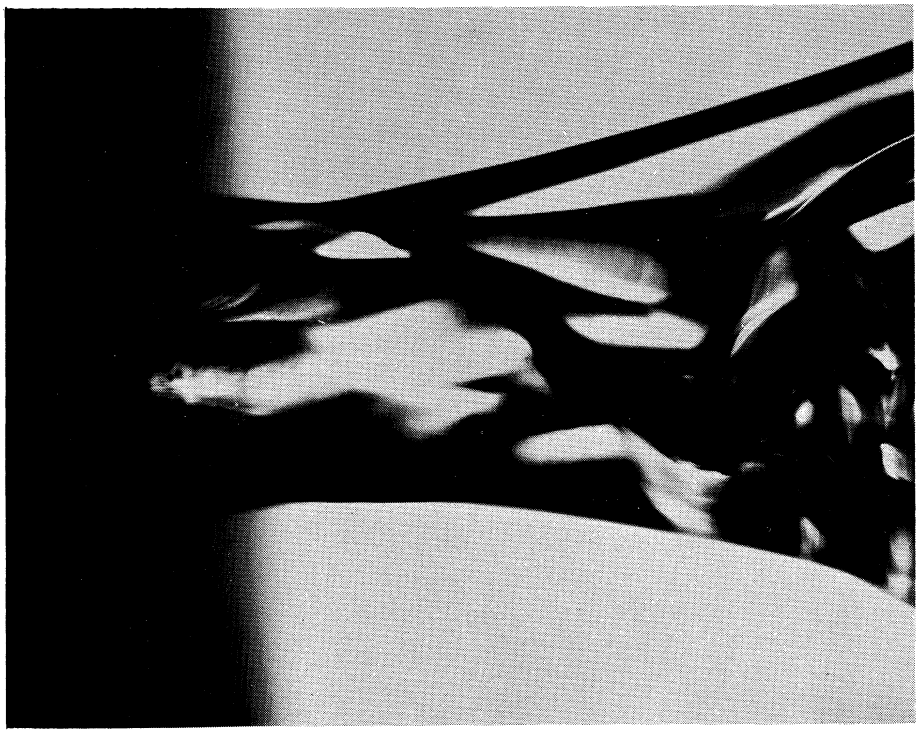

(26)

c. T = 131°F P_{in} = 10 psig

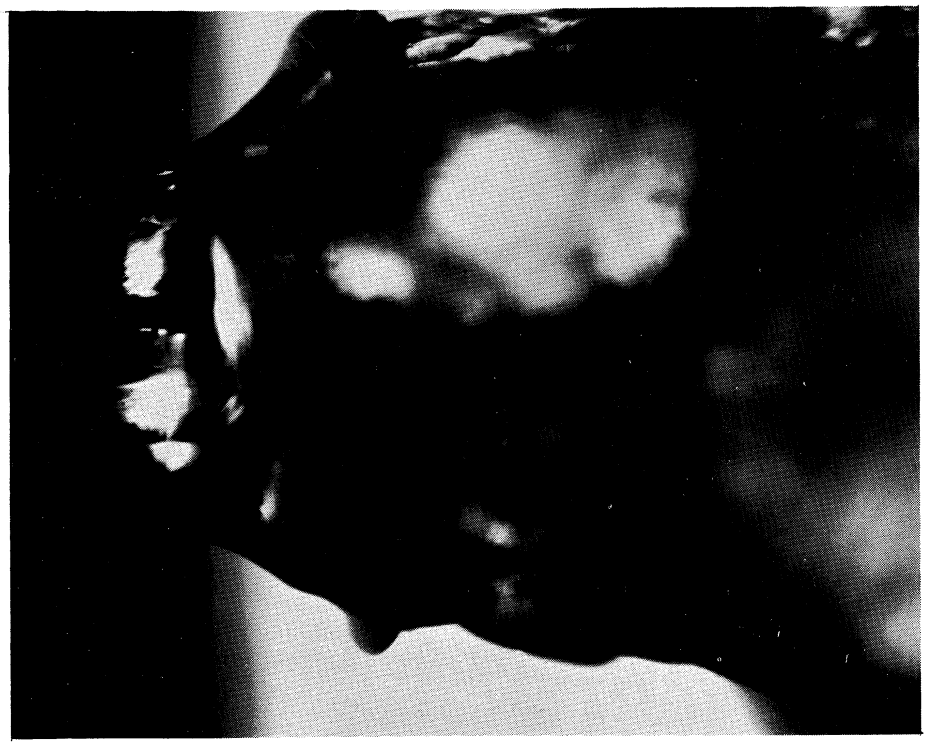

(28)

d. T = 131°F P_{in} = 40 psig

Fig. 8. (Concluded)

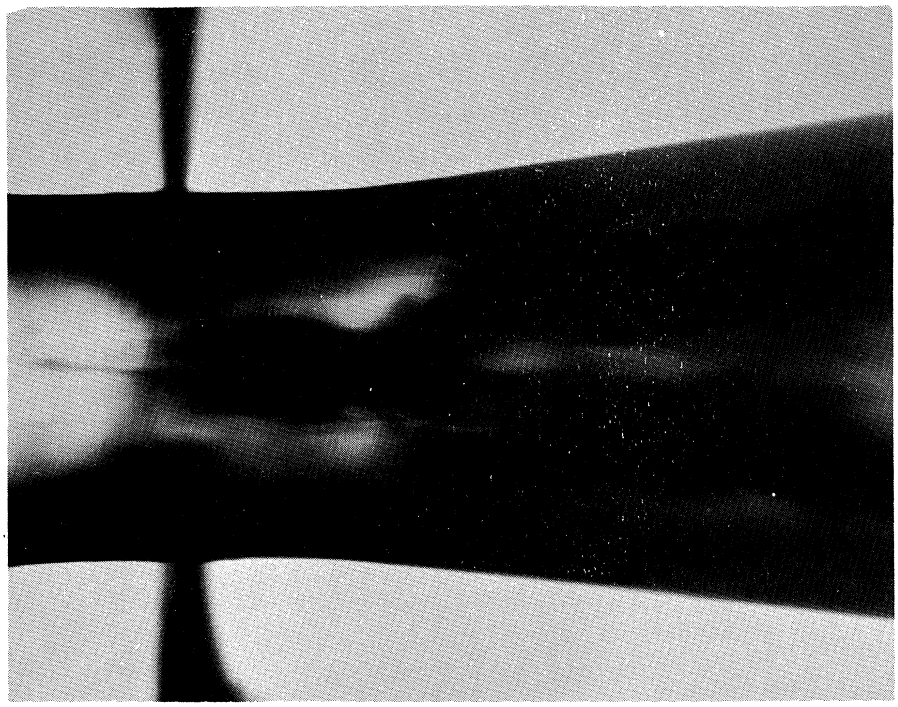

(45)

a. T = 182°F P_{in} = 10 psig
0.205-in. orifice

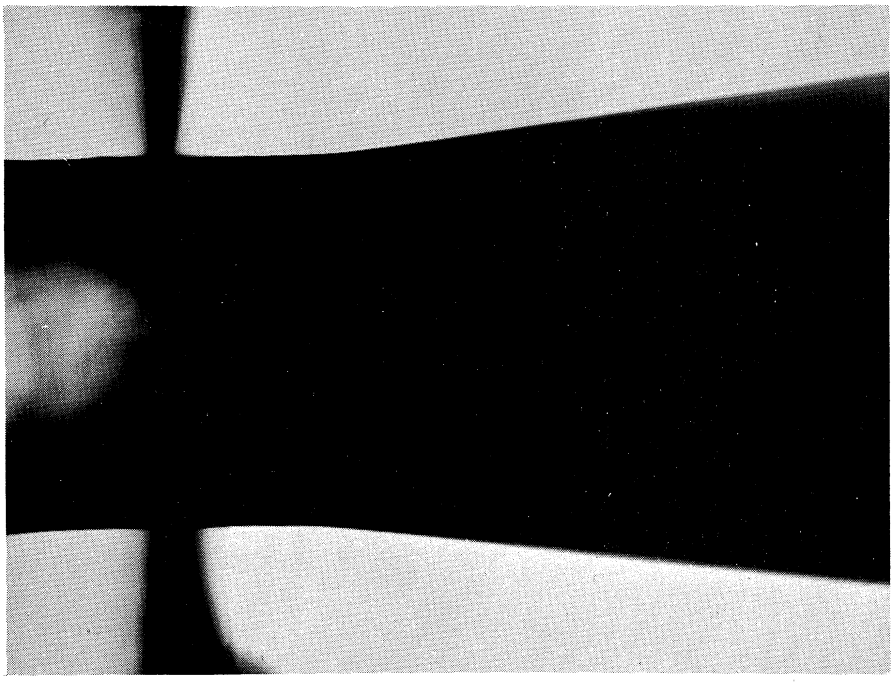

(43)

b. T = 182°F P_{in} = 45 psig
0.205-in. orifice

Fig. 9. Effect of inlet temperature, flow rate, and exit orifice diameter on cavitation (tangential feed).

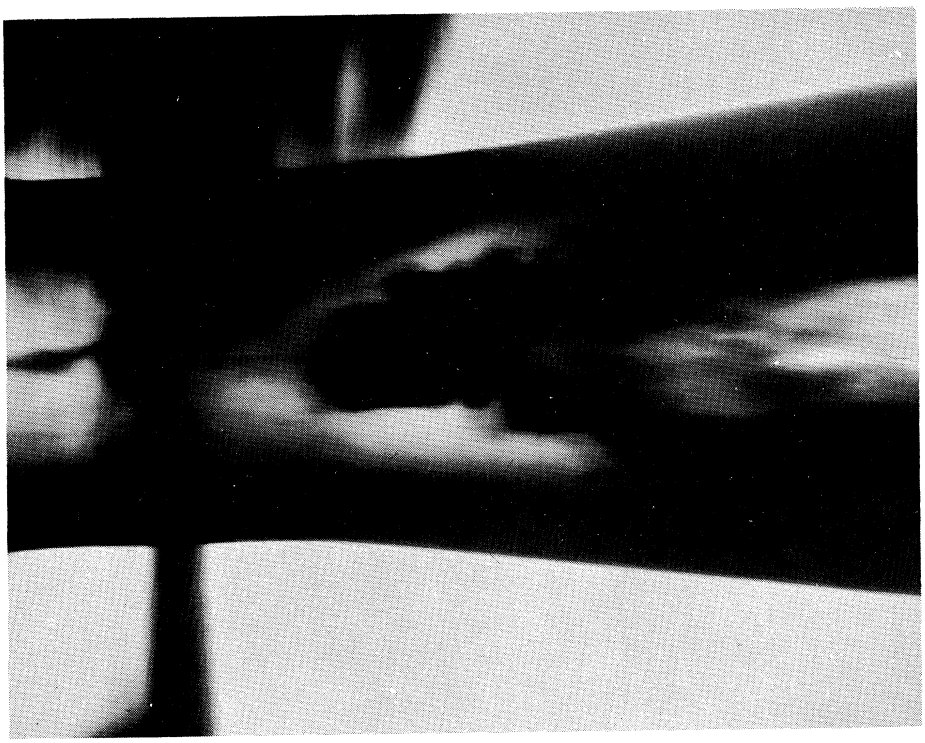

(42)

c. T = 181°F P_{in} = 10 psig
0.120-in. orifice

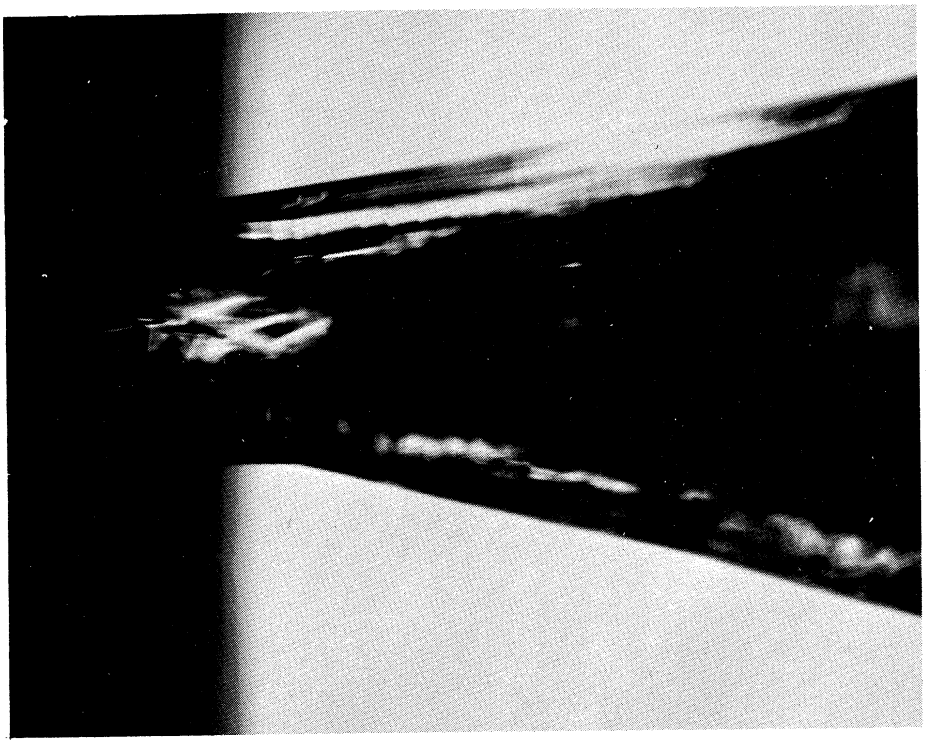

(40)

d. T = 190°F P_{in} = 45 psig
0.120-in. orifice

Fig. 9. (Concluded)

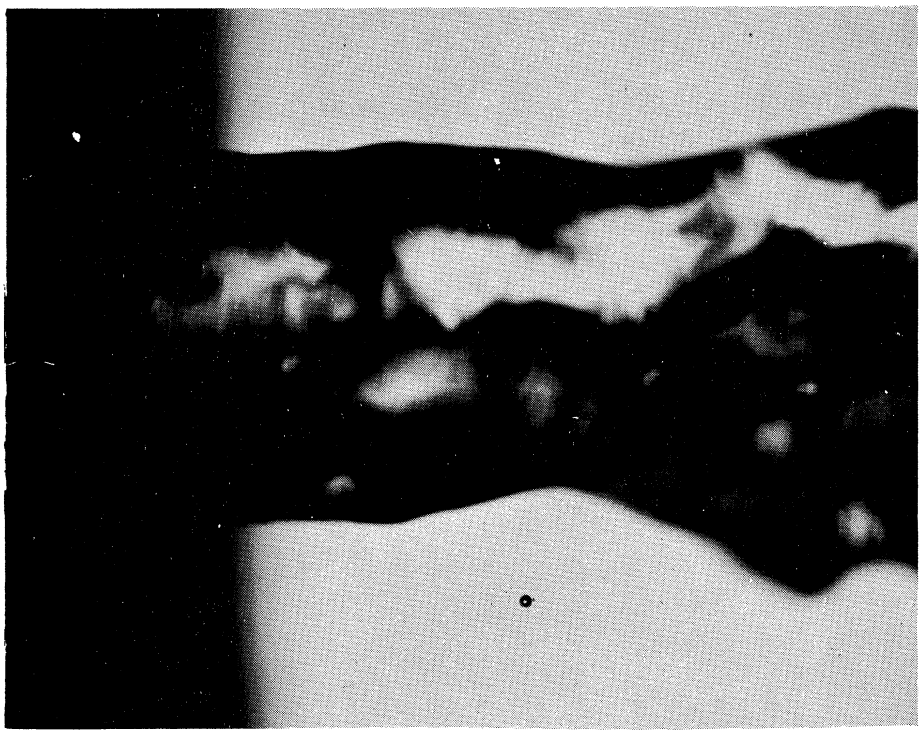

(36)

a. T = 194°F P_{in} = 10 psig
0.205-in. plate

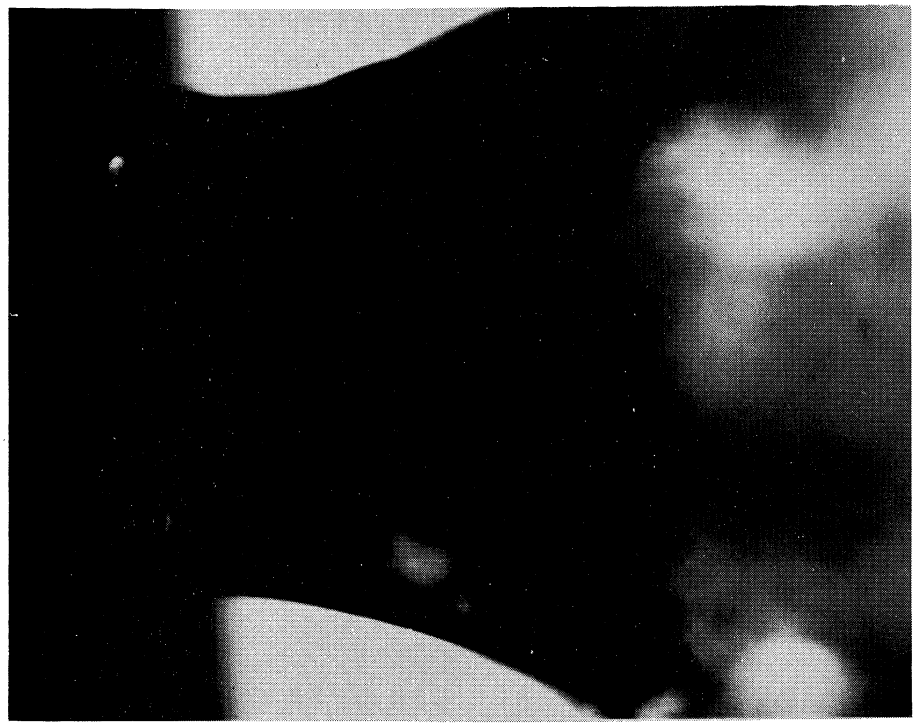

(33)

b. T = 193°F P_{in} = 45 psig
0.205-in. plate

Fig. 10. Effect of cavitation on the free surface of conical jet (tangential feed).

TABLE I

METERING AND PRESSURE DATA ON VENTURI NOZZLE WITH AXIAL WATER FEED

Inlet Pressure, psig	Water Temperature, °F	Throat Pressure, in. Hg Vac.	Flow Rate, lb/min
45	55	28.1	27.0
30	53	28.2	23.7
20	52	28.2	20.8
10*	51	23.9	17.47
45	82	27.9	27.1
30	82	27.5	23.3
20	82	26.9	20.7
10*	80	19.0	17.17
45	115	26.3	26.6
30	114	26.1	22.8
20	114	26.0	20.2
10*	114	20.4	17.0
45	126	25.0	26.3
30	126	24.9	22.9
20	125.5	24.5	20.0
10*	125	19.9	16.78

*Incipient cavitation — critical flow rate.

TABLE II

METERING AND PRESSURE DATA ON VENTURI NOZZLE WITH TANGENTIAL WATER FEED

Inlet Pressure, psig	Water Temperature, °F	Throat Pressure, in. Hg Vac.	Flow Rate, lb/min
45	47	0	23.8
30	46	9	20.5
20	46	11.5	17.85
10	46	11.3	13.84
45	122	3.5 psig	22.3
30	122	2	19.38
20	121	6	16.89
10	120	9	11.47
45	195	11 psig	19.15
30	195	7 psig	15.70
20	194	9 psig	10.26
10	192	4.7 psig	7.37

Runs with tangential water feed showed incipient cavitation at a lower critical flow rate than those with axial water feed. The inlet pressure corresponding to critical flow with tangential water feed was about 6 psig. The upstream boundary of the cavitation zone with tangential feed was observed to migrate from the throat area into the diffuser section as flow was increased above the critical flow rate. With axial feed, this phenomenon was not observed as the upstream boundary of the cavitation zone remained stationary at the diffuser entrance for all flow rates greater than the critical flow rate. Note the increase in throat pressure with increased flow, in contrast with the behavior observed with axial feed.

Additional data have been taken for 0.500-, 0.375-, and 0.250-in. orifices. The effect of the larger orifices was not noticeable. However, for orifices smaller than the venturi throat, flow rates are reduced greatly and throat pressures are increased, approaching the inlet pressure for the smallest orifices.

HYDRAULICS OF FLOW THROUGH CAVITATING VENTURI NOZZLE

The existence of cavitation during experimental runs may be substantiated further by comparing observed throat pressures with those calculated for axial-radial flow of single-phase fluid. The "ideal" pressure at the throat of the venturi may be calculated from the familiar metering relationship shown by Eq. (1):

$$w = \frac{C_V \pi D_2^2}{4} \sqrt{\frac{2g_c(P_1-P_2)\rho}{1-(D_2/D_1)^4}} \quad , \qquad (1)$$

where:

C_V = dimensionless venturi coefficient,
D_2 = diameter of throat,
D_1 = diameter of venturi entrance,
ρ = liquid density,
P_2 = pressure at throat,
P_1 = pressure at inlet,
w = mass flow rate, and
g_c = conversion factor.

The venturi coefficient is normally about 0.98 if the Reynolds number of the fluid flowing at the throat is greater than 10,000. Calculated and measured throat pressures based upon the data for axial water feed (Table I) are presented in Table III.

Calculated and observed throat pressures are seen to agree only for critical flow rates. For higher rates, calculated and observed throat pressures diverge. Inspection of Eq. (1) shows that a larger pressure drop than anticipated can be caused by either a low venturi coefficient or a low fluid density. A low venturi coefficient is not likely, as venturi coefficients are known to increase with increasing Reynolds number, asymptotically approaching a value of 0.98 for Reynolds numbers above 10,000. Low fluid density can result only from two-phase flow near the venturi throat. The calculations of the hydraulics of flow through the venturi nozzle are based upon concepts of single-phase flow. Upon inception of gas nuclei and prior to cavitating implosions, two-phase flow conditions rather than single-phase exist at the throat when the pressure measurements are made. The calculations leading to Table III clearly indicate that the presence of gas phase at the throat accounts for the difference between calculated and observed pressures.

TABLE III

CALCULATED AND OBSERVED THROAT PRESSURES IN VENTURI NOZZLE

w, lb/min	T, °F	P_1, psia	Re_{throat}	$P_{2calc'd}$, psia	P_{2obs}, psia
27.0	55	59.4	68,800	9.7	0.6
23.7	53	44.4	58,500	6.2	0.5
20.8	52	34.4	50,500	4.9	0.5
17.47*	51	24.4	41,800	3.6	2.6
27.1	82	59.4	97,400	9.1	0.7
23.3	82	44.4	83,600	7.2	0.8
20.7	82	34.4	74,500	5.1	1.2
17.7*	80	24.4	60,300	4.2	4.9
26.6	115	59.4	136,500	10.6	1.4
22.8	114	44.4	116,300	8.6	1.5
20.2	114	34.4	103,100	6.3	1.6
17.00*	114	24.4	86,900	4.5	4.3
26.3	126	59.4	150,900	11.6	2.1
22.9	126	44.4	131,400	8.2	2.1
20.0	125.5	34.4	113,600	6.8	2.3
16.78	125	24.4	94,600	4.9	4.5

*Incipient cavitation—critical flow rate.

It is of interest to calculate the relative volumes of liquid and vapor phases present in the vicinity of the venturi throat. If it can be postulated that the actual density ratio between the two-phase fluid mixture and the density of the liquid is approximately equal to the ratio between calculated and observed pressure drops, the following relation may be obtained:

$$\rho_M = \rho_L \frac{(P_1 - P_{2c})}{(P_1 - P_{2o})} \quad , \tag{2}$$

where:

ρ_M = density of two-phase mixture,
ρ_L = density of liquid phase,
P_{2c} = calculated throat pressure,
P_{2o} = observed throat pressure, and
P_1 = inlet pressure.

For one cubic foot of the two-phase mixture the following Eq. (3) may be written by a material balance:

$$\rho_M = x\rho_L + (1-x)\,\rho_G \cong x\rho_L \quad , \tag{3}$$

where:

ρ_G = vapor-phase density (negligible in comparison to ρ_L), and
x = volume fraction liquid in mixture.

Combining Eqs. (2) and (3):

$$x \cong P_1-P_{2c}/P_1-P_{2o} \qquad (4)$$

Calculated volume fractions of liquid and vapor flowing near the throat are presented in Table IV for axial water feed.

TABLE IV

COMPOSITION OF TWO-PHASE MIXTURE AT THE THROAT OF VENTURI NOZZLE

w, lb/min	T, °F	Vol. Fraction Liquid	Vol. Fraction Vapor
27.0	55	0.85	0.15
23.7	53	0.87	0.13
20.8	52	0.87	0.13
17.47*	51	0.95	0.05
27.1	82	0.86	0.14
23.3	82	0.85	0.15
20.7	82	0.88	0.12
17.7*	80	1.0	0
26.6	115	0.84	0.16
22.8	114	0.84	0.16
20.2	114	0.86	0.14
17.00*	114	0.99	0.01
26.3	126	0.83	0.17
22.9	126	0.86	0.14
20.0	125.5	0.86	0.14
16.78*	125	0.98	0.02

*Incipient cavitation—critical flow rate.

The results presented above show a considerable amount of vapor to be present in the vicinity of the throat with super-critical flow rates. In truly cavitating flow the two-phase condition ceases as soon as the vapor bubbles implode in areas of higher pressure. This has been observed to hold in practically all cases of incipient cavitation. When the rates or temperatures are such that pressures much lower than the vapor pressure occur, then some gas phase persists without cavitating throughout the diffuser section. However, for cases observed the amount of vapor entrained out without recollapse is low and most of the gas phase nucleated collapses back into the liquid phase before the fluid leaves the nozzle.

where:

ρ_G = vapor-phase density (negligible in comparison to ρ_L), and
x = volume fraction liquid in mixture.

Combining Eqs. (2) and (3):

$$x \cong P_1-P_{2c}/P_1-P_{2o} \qquad (4)$$

Calculated volume fractions of liquid and vapor flowing near the throat are presented in Table IV for axial water feed.

TABLE IV

COMPOSITION OF TWO-PHASE MIXTURE AT THE THROAT OF VENTURI NOZZLE

w, lb/min	T, °F	Vol. Fraction Liquid	Vol. Fraction Vapor
27.0	55	0.85	0.15
23.7	53	0.87	0.13
20.8	52	0.87	0.13
17.47*	51	0.95	0.05
27.1	82	0.86	0.14
23.3	82	0.85	0.15
20.7	82	0.88	0.12
17.7*	80	1.0	0
26.6	115	0.84	0.16
22.8	114	0.84	0.16
20.2	114	0.86	0.14
17.00*	114	0.99	0.01
26.3	126	0.83	0.17
22.9	126	0.86	0.14
20.0	125.5	0.86	0.14
16.78*	125	0.98	0.02

*Incipient cavitation—critical flow rate.

The results presented above show a considerable amount of vapor to be present in the vicinity of the throat with super-critical flow rates. In truly cavitating flow the two-phase condition ceases as soon as the vapor bubbles implode in areas of higher pressure. This has been observed to hold in practically all cases of incipient cavitation. When the rates or temperatures are such that pressures much lower than the vapor pressure occur, then some gas phase persists without cavitating throughout the diffuser section. However, for cases observed the amount of vapor entrained out without recollapse is low and most of the gas phase nucleated collapses back into the liquid phase before the fluid leaves the nozzle.

The data calculated in Table IV generally confirm experimental observations of increased cavitation with increased flow and elevated temperatures. The good agreement of the calculated and observed throat pressures shown in Table III for critical flow is especially significant. This indicates that visual observation provides accurate means of detecting the onset of cavitation.

The data taken with tangential water feed were not treated in this manner because of the obvious departure from axial-radial flow. With tangential entry the flow becomes truly three-dimensional with axial, radial, and tangential velocity components. It is interesting to note that increasing flow has the opposite effect on throat pressure from that observed with axial flow. This behavior would be expected since the pressure at the throat wall is a measure of the centrifugal force excited by the swirling liquid. Increased flow is accompanied by greater centrifugal force and higher wall pressures result. It is also well known that for a swirling flow the radial pressure distribution is such that one always encounters lowest pressures close to the axis of swirl. This is why the pressure at the axis of the throat is found lower for tangential than for axial water feed. This accounts for the lower critical flow observed for this mode of feed. This also explains the experimental observation that two-phase flow and cavitation occur near the axis of the nozzle rather than at the walls of the nozzle as for axial flow.

The concept of a dimensionless cavitation number has been advanced recently to provide an index for judging the extent of cavitation present in a given flow system. This concept has been used for flow of hot water through orifices in a recent article by F. Numasche, M. Yamabe, and R. Oba, "Cavitation Effect on the Discharge Coefficient of the Sharp-Edged Orifice Plate," ASME Paper 58-A-93. Equation (5) is a standard form of the definition of the cavitation number.

$$K_d = \frac{2g(P_2 - P_d)}{\gamma V_o^2} \qquad (5)$$

where

γ = specific weight of fluid = $\rho\, g/g_c$ lbF/ft^3,
V_o = average throat velocity, ft/sec,
P_2 = pressure at throat, lbF/ft^2,
P_d = vapor pressure of liquid flowing, lbF/ft^2, and
g = acceleration of gravity, ft/sec^2.

Cavitation numbers have been computed using both calculated and observed throat pressures listed in Table III for axial water flow. When calculated pressures were used, cavitation numbers ranged from 0.15 to 0.21. Much smaller cavitation numbers computed from observed pressures are listed in Table V.

Numasche, Yamabe, and Oba have reported that cavitation numbers of 0.25 and lower correspond to cavitating flow through sharp-edged orifices. Probably for the streamlined venturi nozzle a smaller cavitation number would be required for incipient cavitation. In any event the cavitation numbers presented above

TABLE V

CAVITATION NUMBERS DEVELOPED IN VENTURI NOZZLE WITH AXIAL FEED

w, lb/min	T, °F	K_d	w, lb/min	T, °F	K_d
27.0	55	0.008	26.6	115	0
23.7	53	0.009	22.8	114	0.003
20.8	52	0.012	20.2	114	0.006
17.47*	51	0.12	17.00*	114	0.15
27.1	82	0.003	26.3	126	0.001
23.3	82	0.009	22.9	126	0.004
20.7	82	0.021	20.0	125.5	0.021
17.7*	80	0.23	16.78*	125	0.14

*Critical flow--incipient cavitation.

for super-critical flow rates surely correspond to profuse cavitation. Again the calculated data confirm experimental observations of increased cavitation with increased flow and elevated temperatures.

DE-AERATION PHENOMENA

Because the hot tap water used for the experiments described above contains a substantial amount of dissolved air, the creation of sufficiently low pressure zones in the liquid phase probably causes some of this dissolved air to come out of solution. The two-phase zone observed near the throat then probably contained air bubbles in addition to nuclei of water vapor. In those experiments where two-phase flow appears to persist all through the diffuser section, there is a distinct possibility that most of the entrained gas is the air which came out of solution. Because of the fairly slow recovery of the pressure downstream from the throat and due to high fluid velocities encountered, it is believed that the driving force necessary to redissolve air is not large enough to maintain a high rate of diffusion back into the liquid phase. In the runs corresponding to incipient cavitation, where all the evolved gas phase disappears quickly after 1/16 to 1/8 of an inch, with fluid velocities of the order of 50 or more feet per second, it becomes quite clear that resolution of air would require a very high mass-transfer coefficient. The possibility that all the evolved phase is air which came out of solution is thus very remote. This was of concern because resolution of air would be a purely diffusional rate process which probably would not have the abrupt shock effect of implosions on the issuing jet.

CONCLUSIONS

The following conclusions may be deduced from the analysis of the data collected, theoretical calculations performed, and visual observations noted:

1. The insertion of a low-pressure venturi section, upstream of the discharge orifice, does facilitate cavitation at the throat of the nozzle.

2. The effect of cavitation on the jet issuing from the nozzle has been determined photographically by the presence of surface waves which definitely appear to be growing in amplitude.

3. When a cavitating venturi section is integrated into the design of a spray nozzle, it was found experimentally that the diameter of the exit orifice must be slightly larger than the diameter of the throat.

4. The experiments and calculations of flow performed so far indicate that the length of the diffuser section of the venturi may be effectively shortened without drastically affecting the cavitating performance. It is believed that the closer the cavitation location to the issuing jet or spray, the more pronounced the overall effect on the spray produced.

5. Finally, the design of a nozzle cavitating with cold feed is not only possible, but feasible. The cavitating performance definitely disturbs the jet and induces growing waves at its surface.

FUTURE WORK

Little information has been gathered as yet on the effect of cavitation on the properties of spray. A number of photographs have been taken of the orifice effluent, but these have not given drop-size data. Therefore another type of nozzle with a venturi to be used with a Delavan No. 9033 or other similar spray head is being designed. Figure 11 is a sketch of the design of a cavitating venturi adaptor to be fitted with a Delavan nozzle. It is believed that the

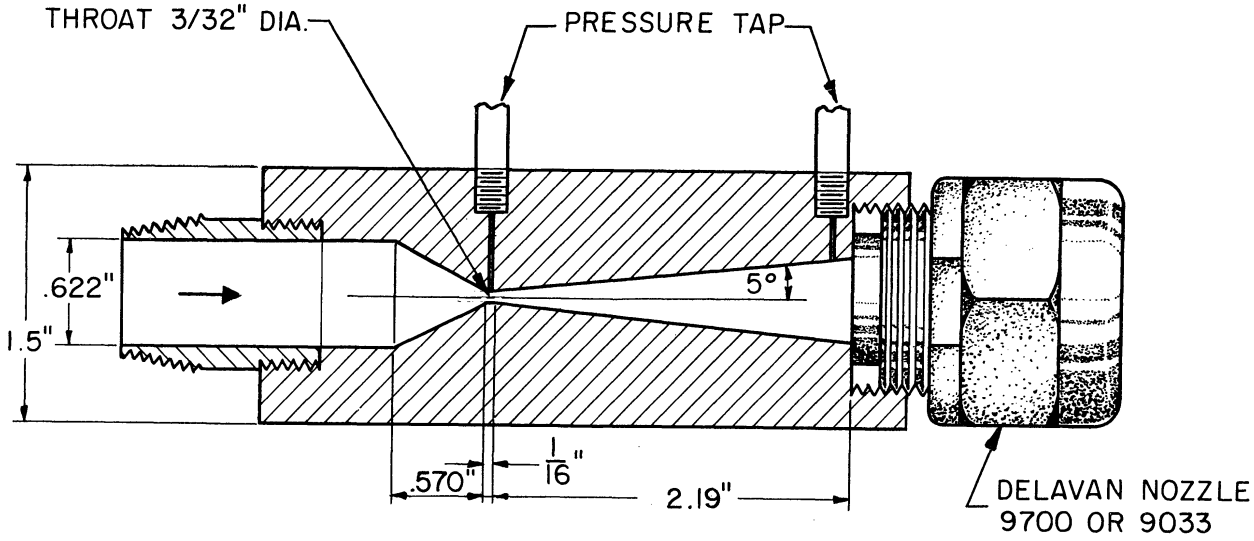

Fig. 11. Sketch of cavitating venturi adaptor, Delavan nozzle assembly.

data obtained from the current nozzle provide a basis for design of a satisfactory cavitating nozzle.

Additional work with the current cavitating nozzle is planned to investigate the effect of diffuser section length upon nozzle performance. Similar runs are anticipated to obtain photographs of the cavitation zone and orifice effluent for both axial and tangential modes of water feed. Also, additional pressure-distribution and flow data will be taken for shorter diffuser sections.

For a complete quantitative evaluation of sprays obtained by cavitating nozzles a series of controlled experiments must be planned and conducted. Data on particle sizes, particle-size distribution, spatial drop distribution, cone angle, and spray penetration will be collected and analyzed with relatively cold feed under both cavitating and noncavitating regimes.

APPENDIX

TABLE A. PRESSURE AT DIFFUSER EXIT
FLOW EQUATION—SINGLE PHASE

Run	w, lb/min	T, °F	μ, lbm/ft-hr	T, °C	Re_{throat}	Re_o	C_o	ρ	ΔP_{psia}	P_{de}
1	27.0	55	2.88	12.8	68,800	42,000	0.61	62.7	0.178	14.55
2	23.7	53	2.97	11.7	58,500	35,700	0.61	62.7	0.137	14.51
3	20.8	52	3.02	11.1	50,500	30,800	0.615	62.7	0.104	14.47
4	17.47	51	3.06	10.5	41,800	25,500	0.62	62.7	0.072	14.44
5	27.1	82	2.04	27.8	97,400	59,400	0.61	62.4	0.183	14.55
6	23.3	82	2.04	27.8	83,600	51,000	0.61	62.4	0.134	14.50
7	20.7	82	2.04	27.8	74,500	45,400	0.61	62.4	0.105	14.47
8	17.17	80	2.09	26.7	60,300	36,800	0.61	62.4	0.073	14.44
9	26.6	115	1.428	46.2	136,500	83,300	0.61	62.0	0.175	14.55
10	22.8	114	1.436	45.6	116,300	71,000	0.61	62.0	0.128	14.50
11	20.2	114	1.436	45.6	103,100	62,900	0.61	62.0	0.101	14.47
12	17.0	114	1.436	45.6	86,900	52,900	0.61	62.0	0.071	14.44
13	26.3	126	1.277	52.2	150,900	92,000	0.61	61.8	0.172	14.54
14	22.9	126	1.277	52.2	131,400	80,200	0.61	61.8	0.130	14.50
15	20.0	125.5	1.290	51.9	113,600	69,200	0.61	61.8	0.099	14.47
16	16.78	125	1.300	51.6	94,600	57,800	0.61	61.8	0.070	14.44

$A_{throat} = (\pi/4)(1/8.12)^2 = 8.53 \times 10^{-5}$ ft^2

$Re = 4w/\pi D\mu$

Atmospheric pressure = 14.37 psia

$D_{throat} = 1/96$ ft

$D_{orifice} = 0.205/12 - D_p = 1.125$ in.

$(D_o/D_p) = 0.182$

Orifice ΔP:

$$w = C_o A_o \sqrt{\frac{2g_c\rho(-\Delta P)}{1-(D_o/D_1)^4}}$$

P_{de} = Press diffuser exit

$$\frac{w^2[1-(D_o/D_1)^4]}{2C_o^2A_o^2g_c\rho} = -\Delta P = \frac{1}{2}\left(\frac{0.61}{C_o}\right)^2\left[\frac{.999}{(.61)^2}\right]\left(\frac{1}{2.29\times10^{-4}}\right)^2\left[\frac{1}{(3600)(32.2)}\right]\frac{w^2}{\rho} = [2.21]\left(\frac{.61}{C_o}\right)^2\left(\frac{w^2}{\rho}\right) \text{ lb/ft}^2$$

$1 - (D_o/D_1)^4 = 1 - .00110 = 0.999$

$\Delta P = (1.533 \times 10^{-2})\left(\frac{.61}{C_o}\right)^2\left(\frac{w^2}{\rho}\right)$ psi

$A_o = 2.29 \times 10^{-4}$ ft^2